Effect of Band Contact on the Temperature Distribution for Dry Friction Clutch

O.I. Abdullah[a], J. Schlattmann[a]

[a]System Technology and Mechanical Design Methodology, Hamburg University of Technology, Germany.

A B S T R A C T

In this study, the two dimensional heat conduction problem for the dry friction clutch disc is modeled mathematically analysis and is solved numerically using finite element method, to determine the temperature field when band contacts occurs between the rubbing surfaces during the operation of an automotive clutch. Temperature calculation have been made for contact area of different band width and the results obtained compared with these attained when complete contact occurs. Furthermore, the effects of slipping time and sliding velocity function are investigated as well. Both single and repeated engagements made at regular interval are considered.

© 2013 Published by Faculty of Engineering

1. INTRODUCTION

Experience shows that most premature clutch failures can be attributed to excessive surface temperature generated during slipping. And to prevent clutch failure before expected lifecycle it is necessary to know the maximum surface temperature and how this depends on known conditions of loading, physical properties and dimensions of the clutch disc and degree of air cooling.

Newcomb [1] derived the equations during slipping period to determine the energy dissipated and the temperatures reached at any instant during a single engagement of a clutch when its torque capacity is a function of time. Two typical torque-time variations are discussed and a comparison is made with the case when the torque is assumed to be constant.

Anderson [2] introduced and discussed four automotive friction system hot spot types. These are asperity, focal, distortional, and regional. Friction material and metal counter surface wear consequences are discussed, as they relate to the different hot spotting types. Focal hot spots are emphasized. These may form martensite on the cast iron drum or disk rubbing surface. Such hot spots, if not prevented, can provide a root cause for unacceptable performance or durability in automotive friction

systems. Computer studies, using a two-dimensional model, are used to complement the experimental studies of critical hot spots and determine hot spot thermal flux limits. Surface melting and known requirements for the formation of martensite are used to establish bounds from the computer analysis.

Lee and Barber [3] investigated the thermoelastic instability in automotive disk brake systems and focusing on the effect of a finite disk thickness. A finite layer model with an anti-symmetric mode of deformation can estimate the onset of instability observed in actual disk brake systems. Also some effects of system parameters on stability are found to agree well to experimental observations.

Lee and Barber [4] investigated thermoelastic instability in an automotive disk brake system experimentally under drag braking conditions. The onset of instability is clearly identifiable through the observation of non-uniformities in temperature measured using embedded thermocouples. A stability boundary is established in temperature/speed space, the critical temperature being attributable to temperature dependence of the brake pad material properties. It is also found that the form of the resulting unstable perturbations or eigen functions changes depending upon the sliding speed and temperature.

Yevtushenko e al [5] were applied one-dimensional transient heat conductivity to study the contact problem of a sliding of two semi-spaces, which induces effects of friction, heat generation and water during braking. In the present temperature analysis the capacity of the frictional source on the contact plane dependent on the time of braking. The problem solved exactly using the Laplace transform technique. Numerical results for the temperature are obtained for the different values of the input parameter, which characterize the duration of the increase of the contact pressure during braking from zero to the maximum value. An analytical formula for the abrasive wear of the contact plane is obtained in the assumption, that the wear coefficient is the linear function of the contact temperature.

Decuzzi and Demelio [6] studied the thermo-mechanical damage of clutches and brakes due to thermoelastic instability (TEI), which leading to

localized surface burning of frictional materials, permanent distortions of metal plates, vibrations and noise. In this work, the analytical formulation proposed before, rephrased in dimensionless form, is employed to estimate the influence of the material properties on the minimum critical speed of sliding systems. Two cases of practical interest are considered, an automotive multi-disc clutch (dissimilar materials case) and a carbon–carbon brake/clutch for high speed applications (similar materials case). In both cases the relative importance in altering the minimum critical speed and the direction of change of each parameter is examined and a comparison with previous available solutions is performed. A simple and sufficiently accurate relation is found to hold between the sliding V or rotating Ω critical speed and the arbitrary material parameter ξ,

$$\frac{V_{\min}}{V_o} = \frac{\Omega_{\min}}{\Omega_o} = \left(\frac{\xi}{\xi_o}\right)^n$$

This can be employed in estimating the optimum set of material properties for sliding systems.

Yun [7] used finite element method to solve the problem involving thermoelasto dynamic instability (TEDI) in frictional sliding systems. The resulting matrix equation contains a complex eigenvalue that represents the exponential growth rate of temperature, displacement, and velocity fields. Compared to the thermoelastic instability (TEI) in which eigenmodes always decay with time when the sliding speed is below a critical value, numerical results from TEDI have shown that some of the modes always grow in the time domain at any sliding speed. As a result, when the inertial effect is considered, the phenomenon of hot spotting can actually occur at a sliding speed below the critical TEI threshold. The finite element method presented here has obvious advantages over analytical approaches and transient simulations of the problem in that the stabilities of the system can be determined for an arbitrary geometry without extensive computations associated with analytical expressions of the contact condition or numerical iterations in the time domain.

Grze [8] investigated the temperature fields of the solid disc brake during short, emergency braking. The standard Galerkin weighted residual algorithm was used to discretize the parabolic heat transfer equation. The finite element simulation

for two-dimensional model was performed due to the heat flux ratio constantly distributed in circumferential direction. Two types of disc brake assembly with appropriate boundary and initial conditions were developed. Results of calculations for the temperature expansion in axial and radial directions are presented. The effect of the angular velocity and the contact pressure evolution on temperature rise of disc brake was investigated. It was found that presented finite element technique for two-dimensional model with particular assumption in operation and boundary conditions validates with so far achievements in this field.

Jing et al [9] studied the disadvantages of the thermo-elastic instability (TEI) due to frictional heat energy at the rough sliding interfaces. The main shortcoming of existing literatures is, in our opinion, that it do not deduce theoretical mathematics model taken into account the rough surface profile with the heat convection and radiation boundary conditions in temperature field. We now present our finite element model that we believe can much reduce this shortcoming. In the full paper, we explain our model in some detail; in this abstract, we just add some pertinent remarks to naming the two topics. Topic 1 is: contact model of rough surface profile. Topic 2 is: temperature field model of brake disks. Finally we perform simulations in ANSYS. The results, shown in the full paper, show the importance of the roughness in the temperature field and the practicability of the model.

Hwang et al [10] determined the temperature distribution, thermal distortion, and thermal stress in a solid disc by three dimensional modeling for repeated braking. Braking is applied four times in the present study; the vehicle is decelerated from 100 to 50 kph with 0.6 g, after which the velocity is again accelerated to 100 kph. In order to simulate the friction heat behavior accurately in repeated braking, the moving heat source, which is defined by time and space variable, is applied on the frictional surface. The temperature field and thermal stress in the disc present a non-uniformity characteristic because of the moving heat source. Temperature and thermal stress of the point on the frictional surface of the brake disc present fluctuation in the braking operation. The coning angle due to the non-uniform radial temperature distribution varies with temperature. Thermal fatigue is also discussed in this article.

Grze [11] developed a transient thermal analysis to examine temperature expansion in the disc and pad volume under simulated operation conditions of single braking process. This complex problem of frictional heating has been studied using finite element method (FEM). The Galerkin algorithm was used to discretize the parabolic heat transfer equation for the disc and pad. FE model of disc/pad system heating with respect to constant thermo-physical properties of materials and coefficient of friction was performed. The frictional heating phenomenon with special reference to contact conditions was investigated.

An axisymmetric model was used due to the proportional relation between the intensity of heat flux perpendicular to the contact surfaces and the rate of heat transfer. The time related temperature distributions in axial and radial directions are presented. Evolution of the angular velocity and the contact pressure during braking was assumed to be nonlinear. Presented transient finite element analysis facilitates to determine temperature expansion in special conditions of thermal contact in axisymmetric model.

Fan et al [12] developed a three-dimensional finite element model for thermal-structure coupling analysis of a type of disc brake was established. And using the direct-coupling technique in finite element method, an emergent working condition of braking process was analyzed, getting the distribution laws of the stress field and the temperature field, and the interacting laws between the stress field and the temperature field. The results correspond to the actual application, thus providing guidance for the designing and the fatigue analysis of disc brakes.

In this paper a finite element method has been applied to calculate the heat generated on the surfaces of friction clutch and temperature distribution for case of bands contact between flywheel and clutch disc, and between the clutch disc and pressure plate (one bad central and two bands) and compared with case of full contact between surfaces for single engagement and repeated engagements. Furthermore, this paper shows effect of pressure capacity on the temperature field, when the pressure is a function of time, three kinds of pressure variation with time (constant, linear and parabolic) are presented.

2. MATHMATICAL MODEL

Consider the basic power transmission shown in Fig. 1, consisting of two inertias I_1 and I_2 initially rotating at unequal angular velocities Ω_1 and Ω_2 and at any instant time t, rotating at different angular velocities ω_1 and ω_2 respectively throughout the clutch engagement. The moment of inertias for input and output are I_1 and I_2. And T_1 is input torque and T_2 is output torque. During slipping the torque capacity of the clutch varies as a function of time ϕ (t). It assumed that the torques T_1 and T_2 are constant since any variation in these values is likely to be small compared to the uncertainty of their measured values. Then the equations of motion for the system are expressed as follows [1]:

$$T_1 - \phi(t) = I_1 \frac{d\omega_1}{dt} \qquad (1)$$

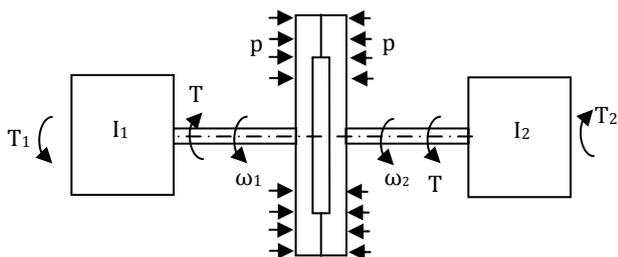$$\phi(t) - T_2 = I_2 \frac{d\omega_2}{dt} \qquad (2)$$

Fig. 1 Basic power transmission system.

Integrating Eq (1) and Eq (2), and using the initially conditions (at t=0, ω_1=Ω_1 and ω_2=Ω_2), where Ω_1 and Ω_2 are the angular velocity initially for flywheel and output end of shaft respectively:

$$\omega_1 = \frac{T_1}{I_1} t - \frac{1}{I_1} \int_0^t \phi(t)\, dt + \Omega_1 \qquad (3)$$

$$\omega_2 = -\frac{T_2}{I_2} t - \frac{1}{I_2} \int_0^t \phi(t)\, dt + \Omega_2 \qquad (4)$$

And the relative angular velocity (ω_r=ω_1- ω_2) is:

$$\omega_r = M\, t - P \int_0^t \phi(t)\, dt + \omega_{ro} \qquad (5)$$

where:

$$M = \frac{T_1}{I_1} + \frac{T_2}{I_2},\, P = (\frac{1}{I_1} + \frac{1}{I_2})\, \text{and}\, \omega_{ro} = \Omega_1 - \Omega_2$$

If there is no external torques (M=0), then the eq. (5) will be:

$$\omega_r = -P \int_0^t \phi(t)\, dt + \omega_{ro} \qquad (6)$$

The slipping period ts determined by putting (ω_r=0) in eq. (6) yield:

$$\omega_{ro} = P \int_0^t \phi(t)\, dt \qquad (7)$$

The simplest torques (under uniform wear condition) variation with time during slipping [1]:

1. Constant torque (or pressure)

The pressure for this case is:

$$p_{max}(t) = p_{max\, o} \qquad (8)$$

then:

$$\phi(t) = T_o = p_{max}(t)\, \mu\, \pi\, r_i\, (r_o^2 - r_i^2) = C_o \qquad (9)$$

where: $C_o = \mu\, \pi\, p_{max\, o}\, r_i\, (r_o^2 - r_i^2)$

And it can be found the slipping time t_s from Eq. (7), and relative angular velocity ω_r form Eq. (6):

$$t_s = \frac{\omega_{ro}}{P T_o} \qquad (10)$$

$$\omega_r(t) = \omega_{ro}(1 - \frac{t}{t_s}) \qquad (11)$$

2. Pressure increasing linearly

The pressure function is:

$$p_{max}(t) = p_{max\, o}\, (t/t_s) \qquad (12)$$

then:

$$\phi(t) = T_o\, (t/t_s) = \\ \mu\, \pi\, p_{max\, o}\, (t/t_s)\, r_i\, (r_o^2 - r_i^2) = C_o\, (t/t_s) \qquad (13)$$

By the same procedures in item (1) it can be fund the slipping time and relative angular velocity:

$$t_s = \frac{2\, \omega_{ro}}{P T_o} \qquad (14)$$

$$\omega_r(t) = \omega_{ro}\left(1 - \left(\frac{t}{t_s}\right)^2\right) \qquad (15)$$

3. Pressure parabolically increasing

The pressure function is:

$$p_{\max}(t) = p_{\max o}(t/t_s)\{2-(t/t_s)\} \qquad (16)$$

then,

$$\phi(t) = T_o(t/t_s)\{2-(t/t_s)\} =$$
$$\mu \pi p_{\max o}(t/t_s)\{2-(t/t_s)\}r_i(r_o^2-r_i^2) = \quad (17)$$
$$C_o(t/t_s)\{2-(t/t_s)\}$$

The slipping time and relative angular velocity are:

$$t_s = \frac{3\omega_{ro}}{2PT_o} \qquad (18)$$

$$\omega_r(t) = \omega_{ro}\left(\frac{1}{2}\left(\frac{t}{t_s}\right)^3 - \frac{3}{2}\left(\frac{t}{t_s}\right)^2 + 1\right) \qquad (19)$$

During the slipping period, the thermal heat fluxes with time on the clutch at any instant per unit area (W/m²) is [11]:

$$q(t) = f_c \mu\, p(t)\omega(t)r_i \qquad (20)$$

where f_c is the heat partition ratio which imposes division of heat entering the clutch, pressure plate and flywheel (assume the same material properties for the flywheel and pressure plate), and is given as follows [12].

$$f_c = \frac{\sqrt{K_c\,\rho_c\,c_c}}{\sqrt{K_c\,\rho_c\,c_c}+\sqrt{K_f\,\rho_f\,c_f}} =$$
$$\frac{\sqrt{K_c\,\rho_c\,c_c}}{\sqrt{K_c\,\rho_c\,c_c}+\sqrt{K_p\,\rho_p\,c_p}} \qquad (21)$$

where k is the thermal conductivity, ρ is the density and c is the specific heat. All values and parameters, which refer to the axial cushion, friction material, flywheel and pressure plate in the following considerations, will have bottom indexes cu, c, f and p respectively. Then, the heat flux on the clutch disc for constant pressure is:

$$q(t) = f_c \mu\, p_{\max o}\,\omega_{ro}\,r_i\left(1-\frac{t}{t_s}\right) \qquad (22)$$

The heat flux on the clutch disc for linear pressure is:

$$q(t) = f_c \mu\, p_{\max o}\,\omega_{ro}\,r_i\left(\frac{t}{t_s}-\left(\frac{t}{t_s}\right)^3\right) \qquad (23)$$

And the heat flux on the clutch disc for parabolic pressure is:

$$q(t) = f_c \mu\, p_{\max o}\,\omega_{ro}\,r_i\,*$$
$$\left(\begin{array}{c}2\left(\dfrac{t}{t_s}\right)-\left(\dfrac{t}{t_s}\right)^2-3\left(\dfrac{t}{t_s}\right)^3\\[2mm]+\dfrac{5}{2}\left(\dfrac{t}{t_s}\right)^4-\dfrac{1}{2}\left(\dfrac{t}{t_s}\right)^5\end{array}\right) \qquad (24)$$

The maximum heat fluxes occur at (t=0), $\{t=(t_s/\sqrt{3})\}$ and (t=0.467 t_s) corresponding to the constant pressure, linear pressure and parabolic pressure respectively.

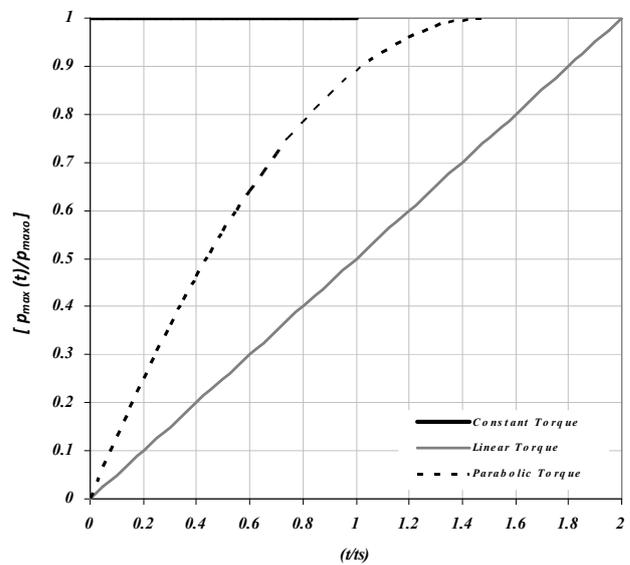Figs. 2, 3 and 4 shows the pressure, relative slip speed and heat flux varies with time during the slipping.

Fig. 2. Variation of [$p_{\max}$(t)/$p_{\max o}$] with time for constant, linearly and parabolically increasing torque. (t_s is the slipping time when the torque is constant).
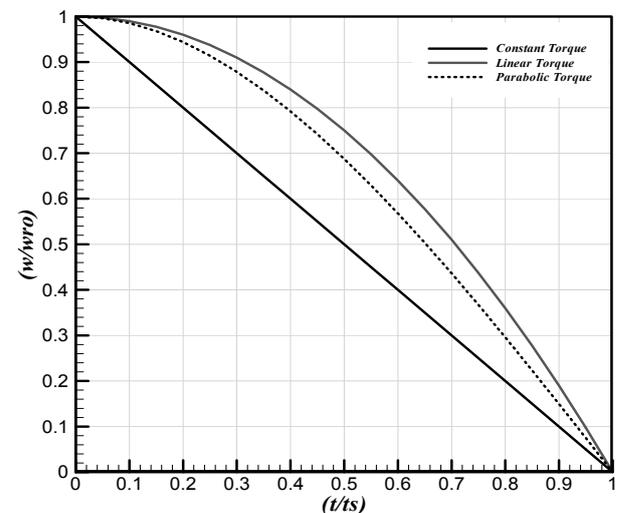

Fig. 3 Variation of [ω_r(t)/ω_{ro}] with (t/t_s) for constant, linearly and parabolically increasing torque.
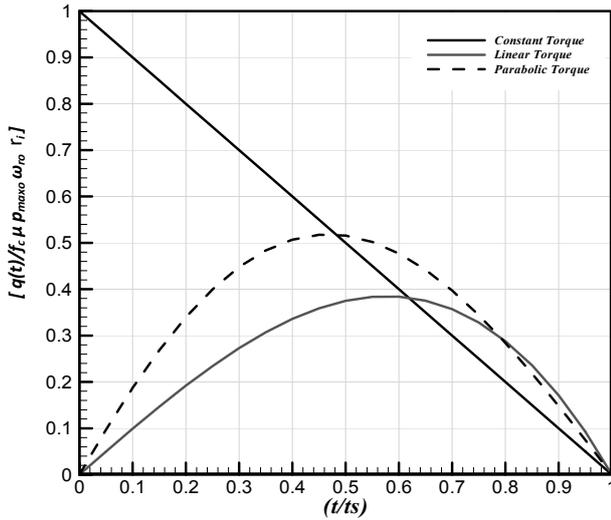
321

Fig. 4 Variation of $[q(t)/f_c\,\mu\,p_{maxo}\,\omega_{ro}\,r_i]$ with (t/t_s) for constant, linearly and parabolically increasing torque.

The total thermal energy dissipated during a single engagement for constant pressure is:

$$Q_{Tc} = \frac{1}{2} f_c\, r_i\, A\, \mu\, p_{\max o}\, \omega_{ro}\, t_s \qquad (25)$$

where, A $[A = n\,\pi\,(r_o^2 - r_i^2)]$ is the total area for contact and n number of contact surfaces. The total thermal energy during a single engagement for linear pressure is:

$$Q_{Tl} = \frac{1}{4} f_c\, r_i\, A\, \mu\, p_{\max o}\, \omega_{ro}\, t_s \qquad (26)$$

And the total thermal energy during a single engagement for parabolic pressure is:

$$Q_{Tp} = \frac{1}{3} f_c\, r_i\, A\, \mu\, p_{\max o}\, \omega_{ro}\, t_s \qquad (27)$$

When the engagement process starts for clutch, the heat will generated between the surfaces due to the slipping (result of the difference in velocities between the driving shaft and driven shaft). The heat generated will dissipate by the conduction between friction clutch components and by convection to environment. Due to short time for slipping process the radiation is neglected. It can be obtained, that the temperature distribution by building two-dimensional models to present the frictional heating process for friction clutch. The starting point for the analysis of the temperature field in the friction clutch is the parabolic heat conduction equation in the cylindrical coordinate system {r-radial coordinate (m), θ-circumferential coordinate (rad), and z-axial coordinate (m)} [13], which is centered in the axis of the disc and z points to it's thickness (Fig. 5-a).

$$\frac{\partial^2 T}{\partial r^2} + \frac{1}{r}\frac{\partial T}{\partial r} + \frac{1}{r^2}\frac{\partial^2 T}{\partial \theta^2} + \frac{\partial^2 T}{\partial z^2} = \frac{1}{\alpha}\frac{\partial T}{\partial t};$$
$$r_i \leq r \leq r_o, 0 \leq \theta \leq 2\pi, 0 \leq z \leq \delta, t > 0 \qquad (28)$$

where α is the thermal diffusivity, α=k/ρ c, r_i and r_o are the inner and outer radius for of the clutch disc. Hence the distribution of heat flow will be uniform in circumferential direction, which means that, the temperature and heat flow will not vary in θ direction, and thus the heat conduction equation reduces to:

$$\frac{\partial^2 T}{\partial r^2} + \frac{1}{r}\frac{\partial T}{\partial r} + \frac{\partial^2 T}{\partial z^2} = \frac{1}{\alpha}\frac{\partial T}{\partial t};$$
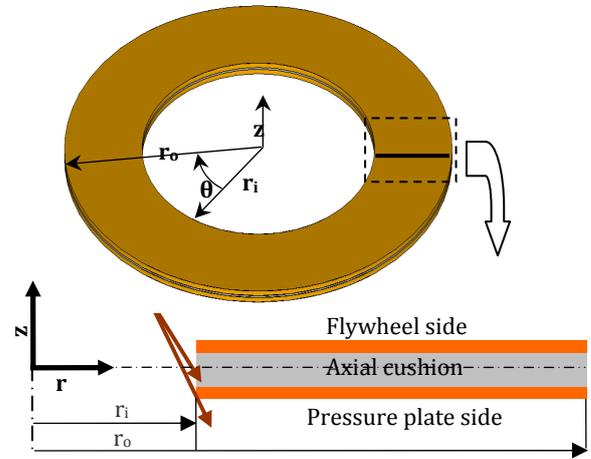$$r_i \leq r \leq r_o, 0 \leq z \leq \delta, t > 0 \qquad (29)$$

Fig. (5-a). The friction clutch disc (axisymmetric).

The boundary and initial conditions are given as follows for all cases during engagement:

$$K_{cu}\frac{\partial T}{\partial r}\Big|_{r=r_0} = h[T(r_o, z, t) - T_a];$$
$$0 \leq z \leq t_{cu}/2,\ t \geq 0 \qquad (30)$$

where T_a is the ambient temperature and h is the convection heat transfer coefficient.

$$K_c\frac{\partial T}{\partial r}\Big|_{r=r_0} = h[T(r_o, z, t) - T_a];$$
$$(t_{cu}/2) \leq z \leq (t_{cu}/2) + t_c, t \geq 0 \qquad (31)$$

$$K_c\frac{\partial T}{\partial r}\Big|_{r=r_i} = h[T(r_i, z, t) - T_a];$$
$$(t_{cu}/2) \leq z \leq,(t_{cu}/2) + t_c,\ t \geq 0 \qquad (32)$$

The initial temperature is,

$$T(r, \theta, z, 0) = T_i;$$
$$r_i \leq r \leq r_o,\ 0 \leq z \leq t_c + (t_{cu}/2) \qquad (33)$$

$$\frac{\partial T}{\partial r}\Big|_{r=r_i} = 0; \quad 0 \le z \le (t_{cu}/2), \; t \ge 0 \quad (34)$$

$$\frac{\partial T}{\partial z}\Big|_{z=0} = 0; \quad r_i \le r \le r_o, \; t \ge 0 \quad (35)$$

The boundary condition for contact surface, for the first case (full contact area) is (Fig. 5-b),

$$K_c \frac{\partial T}{\partial z}\Big|_{z=(t_{cu}/2)+t_c} = q_c(t);$$
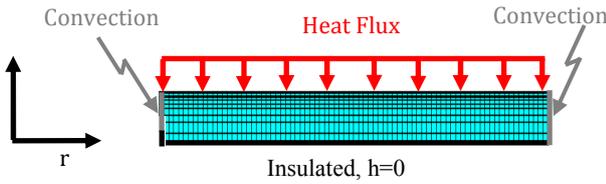$$r_i \le r \le r_o, \; 0 \le t \le t_s \quad (36)$$

Fig. (5-b). FE model with boundary conditions for case (1).

For the second and third cases (one central band of contact), the boundary conditions for contact surface are (Fig. 5-c),

$$K_c \frac{\partial T}{\partial z}\Big|_{z=(t_{cu}/2)+t_c} = 0;$$
$$r_i \le r < r_1, r_2 < r \le r_o \; 0 \le t \le t_s \quad (37)$$

$$K_c \frac{\partial T}{\partial z}\Big|_{z=(t_{cu}/2)+t_c} = q_c(t);$$
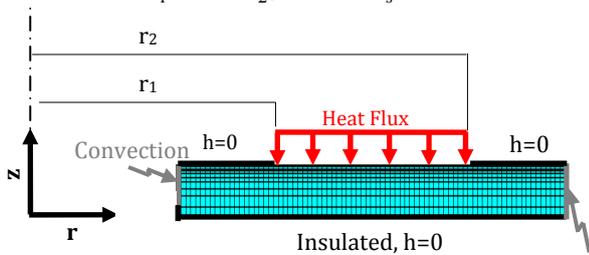$$r_1 \le r \le r_2, \; 0 \le t \le t_s \quad (38)$$

Fig. (5-c). FE model with boundary conditions for cases (2 & 3).

For the fourth and fifth cases (two band of rubbing contact), the boundary conditions for contact surface are (Fig. 5-d),

$$K_c \frac{\partial T}{\partial z}\Big|_{z=(t_{cu}/2)+t_c} = q_c(t);$$
$$r_i \le r \le r_1, r_2 \le r \le r_o, \; 0 \le t \le t_s \quad (39)$$

$$K_c \frac{\partial T}{\partial z}\Big|_{z=(t_{cu}/2)+t_c} = 0;$$
$$r_1 < r < r_2, \; 0 \le t \le t_s \quad (40)$$
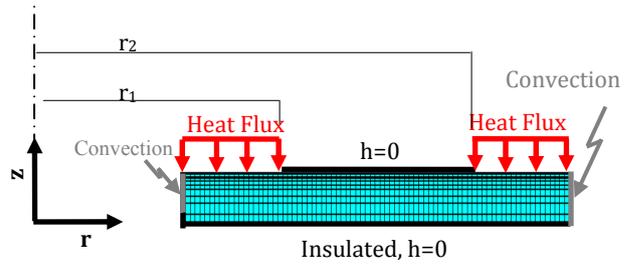

Fig. (5-d). FE model with boundary conditions for cases (4 & 5).

The details of each the case is outlined in Table (1).

Table 1. Description of r_1 and r_2 for all cases.

Case No.	Description	Contact area %
1	Full contact: r_1=-, r_2=-	100
2	One band of contact: $r_1 = \sqrt{\dfrac{r_i^2 + r_i r_o}{2}}, r_1 = \sqrt{\dfrac{r_o^2 + r_i r_o}{2}}$	50
3	One band of contact: $r_1 = \sqrt{\dfrac{-r_o^2 + 4 r_i r_o + 5 r_i^2}{8}}$ $r_2 = \sqrt{\dfrac{5 r_o^2 + 4 r_i r_o - r_i^2}{8}}$	75
4	Two bands of contact: $r_1 = \sqrt{0.25 r_o^2 + 0.75 r_i^2}$ $r_2 = \sqrt{0.75 r_o^2 + 0.25 r_i^2}$	50
5	Two bands of contact: $r_1 = \sqrt{\dfrac{3 r_o^2 + 5 r_i^2}{8}}$ $r_2 = \sqrt{\dfrac{5 r_o^2 + 3 r_i^2}{8}}$	100

3. FINITE ELEMENT FORMULATION

The object of this section is to develop approximate time-stepping procedures for axisymmetric transient governing equations. For this to happen, the following boundary and initial conditions are considered:

$$T = T_p \quad on \; \Gamma_T \quad (41)$$

$$q = -h(T - T_a) \; on \Gamma_h \quad (42)$$

$$q = q_{cu} \quad on \; \Gamma_q \quad (43)$$

323

$$T = T_o \ on \ time \quad t = 0 \tag{44}$$

where T_p is the prescribed temperature, $\Gamma_T, \Gamma_h, \Gamma_q$, are arbitrary boundaries on which temperature, convection and heat flux are prescribed. In order to obtain matrix form of Eq. (25) the application of standard Galerkin's approach was conducted [15]. The temperature was approximated over space as follows:

$$T(r,z,t) = \sum_{i=1}^{n} N_i(r,z) T_i(t) \tag{45}$$

where: Ni are shape functions, n is the number of nodes in an element, Ti(t) are time dependent nodal temperatures. The standard Galerkin's approach of Eq. (25) leads to the following equation:

$$\int_{\Omega} K N_i \left[\frac{\partial^2 T}{\partial r^2} + \frac{1}{r}\frac{\partial T}{\partial r} + \frac{\partial^2 T}{\partial z^2} - \rho C \frac{\partial T}{\partial t} \right] d\Omega = 0 \tag{46}$$

Using integration by parts of Eq. (42) we obtain,

$$-\int_{\Omega} K \left[\begin{array}{c} \frac{\partial N_i}{\partial r}\frac{\partial T}{\partial r} + \frac{\partial N_i}{\partial z}\frac{\partial T}{\partial z} - \frac{N_i}{r}\frac{\partial T}{\partial r} + \\ N_i \rho C \frac{\partial T}{\partial t} \end{array} \right] d\Omega \tag{47}$$
$$+ \int_{\Gamma} K N_i \frac{\partial T}{\partial r} l \, d\Gamma + \int_{\Gamma} K N_i \frac{\partial T}{\partial z} n \, d\Gamma = 0$$

Integral form of boundary conditions:

$$\int_{\Gamma} K N_i \frac{\partial T}{\partial r} l d\Gamma + \int_{\Gamma} K N_i \frac{\partial T}{\partial z} n \, d\Gamma = \\ -\int_{\Gamma_q} N_i \, q \, d\Gamma_q - \int_{\Gamma_h} N_i \, h (T - T_a) \, d\Gamma_h \tag{48}$$

Substituting Eq. (44) and spatial approximation Eq. (41) to Eq. (43) we obtain:

$$-\int_{\Omega} K \left[\frac{\partial N_i}{\partial r}\frac{\partial N_j}{\partial r} + \frac{\partial N_i}{\partial z}\frac{\partial N_j}{\partial z} - \frac{N_i}{r}\frac{\partial N_j}{\partial r} \right] T_j d\Omega$$
$$-\int_{\Omega} \rho C N_i \frac{\partial N_j}{\partial t} T_j \, d\Omega - \int_{\Gamma_q} N_i \, q \, d\Gamma_q \tag{49}$$
$$-\int_{\Gamma_h} N_i \, h (T - T_a) d\Gamma_h = 0$$

where, i and j represent the nodes. Equation (45) can be written in matrix form:

$$[C]\left\{ \frac{\partial T}{\partial t} \right\} + [K][T] = \{R\} \tag{50}$$

Where [C] is the heat capacity matrix, [K] is the heat conductivity matrix, and {R} is the thermal force matrix, or:

$$[C_{ij}]\left\{ \frac{\partial T_j}{\partial t} \right\} + [K_{ij}][T_j] = \{R_j\} \tag{51}$$

where,

$$[C_{ij}] = \int_{\Omega} \rho C N_i N_j \, d\Omega$$

$$[K_{ij}] = \int_{\Omega} K \left(\begin{array}{c} \frac{\partial N_i}{\partial r}\frac{\partial N_j}{\partial r}\{T_j\} + \frac{\partial N_i}{\partial z}\frac{\partial N_j}{\partial z}\{T_j\} \\ -\frac{N_i}{r}\frac{\partial N_j}{\partial r}\{T_j\} \end{array} \right) d\Omega +$$
$$\int_{\Gamma} h N_i N_j d\Gamma$$

$$[R_i] = -\int_{\Gamma_q} q N_i \, d\Gamma_q + \int_{\Gamma_h} N_i \, h T_a \, d\Gamma_h$$

or in matrix form,

$$[C] = \int_{\Omega} \rho C [N]^T [N] d\Omega$$

$$[K] = \int_{\Omega} K [B]^T [D][B] d\Omega + \int_{\Gamma} h [N]^T [N] d\Gamma$$

$$\{R\} = -\int_{\Gamma_q} q [N]^T \, d\Gamma_q + \int_{\Gamma_h} h T_a [N]^T \, d\Gamma_h$$

Table 2. Thermophysical properties of materials and operations conditions for the thermal analysis.

Parameters	Values
Inner radius, r_i [m]	0.085
Outer radius, r_o [m]	0.135
Moments of inertia for the engine [kg-m²]	1
Moments of inertia for the transmission/vehicle [kg-m²]	5
Torque T [Nm]	587.47
Thickness of friction material, t_c [m]	0.002
Thickness of the axial cushion, t_{cu} [m]	0.001
Maximum pressure, p_{maxo} [MPa]	0.25
Coefficient of friction, μ	0.4
Number of friction surfaces, n	2
Maximum angular slipping speed, ω_{ro} (rad/sec)	220
Conductivity for friction material, K_c (W/mK)	0.75
Conductivity for pressure plate & flywheel, K_p & K_f (W/mK)	56
Density for friction material, ρ_c (kg/m³)	1300
Density for pressure plate & flywheel, ρ_p & ρ_f (kg/m³)	7200
Specific heat for friction material, c_c (J/kgK)	1400
Specific heat for pressure plate & flywheel, c_p & c_f (J/kgK)	450
Time step, Δt (s)	0.002
The slipping time (constant pressure), t_{s1}	0.3121
The slipping time (linear pressure), t_{s2}	0.624
The slipping time (parabolic pressure), t_{s3}	0.468

In order to determine temperature distribution of this transient heat conduction problem, the fine mesh element was essential. Moreover, when the iterative method of the given problem is employed, then a relatively short time is needed for the calculations. In the next step of the study, the Crank-Nicolson method was selected as an unconditionally stable scheme. In this paper ANSYS software was used to investigate transient thermoelastic analysis behaviour of dry friction clutch. In all computations for the friction clutch model, it has been assumed a homogeneous and isotropic material and all parameters and materials properties are listed in Table 2.

The heat transfer coefficient was changed as function of the relative surface velocity according to Balazs et al [14], in a stationary position, the value specified was (5W/m² K), and at 1500 r.p.m 15, 20 ,35 and 40 W/(m² K) as a function of the relative surface speed in m/s. The eight-noded thermal element (PLANE77) was used in this analysis; the element has one temperature degree of freedom at each node as the temperature is scalar. A mesh sensitivity study was done to choose the optimum mesh from computational accuracy point of view.

4. RESULTS AND DISCUSSIONS

In this paper the temperature distribution of the friction clutch disc for the bands contact has been investigated. Five cases involving different regions and percentage area of rubbing in contact have been considered, with assuming for each configuration dissipating the same total energy during an engagement. Full contact of area of clutch disc for the first case, 50 % and 75 % of central band contact area is considered for case 2 and case 3 respectively, whereas the two bands of 50 % and 75 % contact area used for case 4 and case 5 respectively.

Figure 6 presents the variation of temperature with time for single engagement and different types of pressure (case-2) at mean radius rm. It can be seen from this figure that the maximum effect on temperature change occurs when applied constant pressure. The maximum ratio for temperature differences for ($\Delta_{const. pressure}/\Delta_{linear pressure}$) and ($\Delta_{const. pressure}/\Delta_{parabolic pressure}$) are found to be 1.24 and 1.1 respectively.
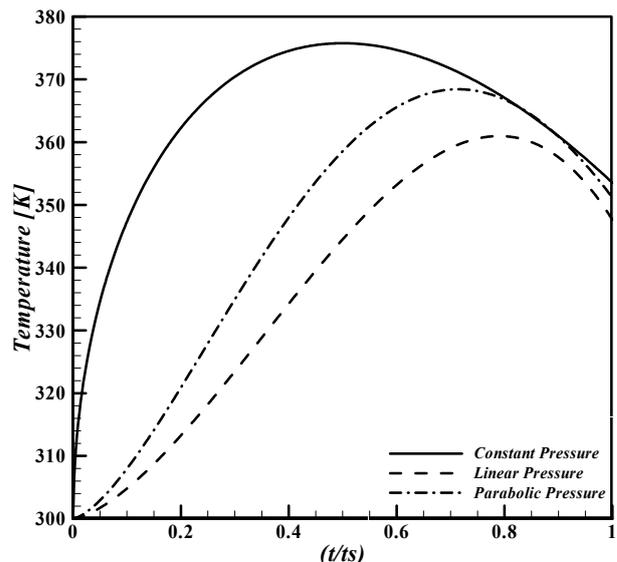

Fig. 6. Variation of temperature with time at r_m (Case 2).

Figures 7, 8 and 9 demonstrate the variation of surface temperatures with time for different contact area and different types of pressure. In all figures, it was observed that the temperature increases when the contact area decreases (pressure increases). The temperature is proportional to the applied pressure and time of slipping, and the temperature increases when the slipping time and contact area decrease. When the contact area decreases from 100 % to 50 % the maximum increases in the difference temperature is approximately 50 % for all types of pressures.
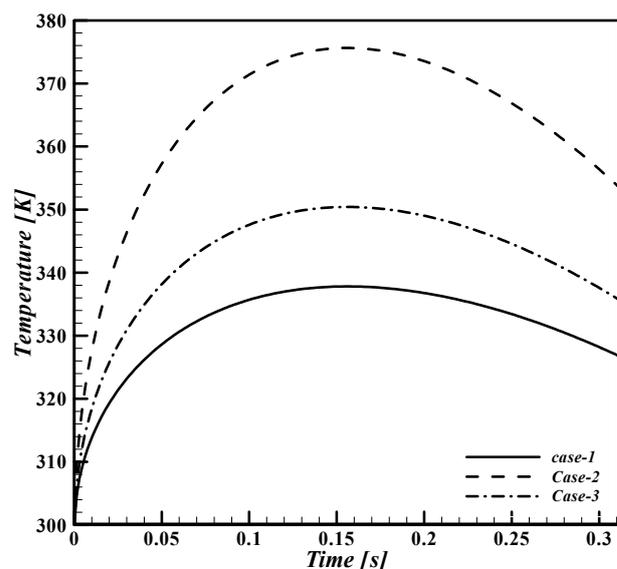

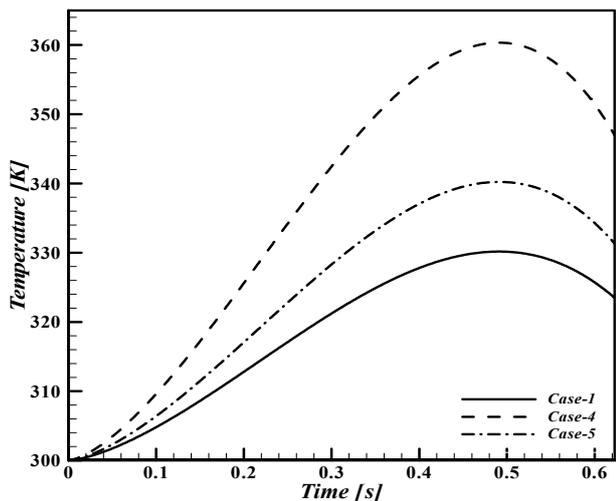**Fig. 7.** Variation of temperature with time at r_m (Constant pressure).

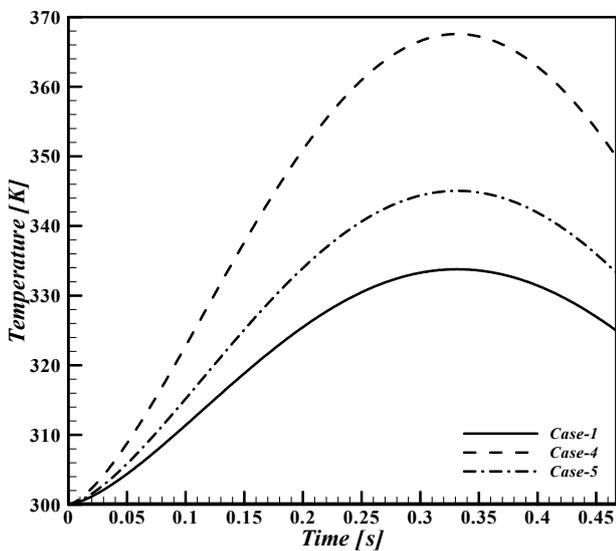**Fig. 8.** Variation of temperature with time at r_i (Linear pressure).

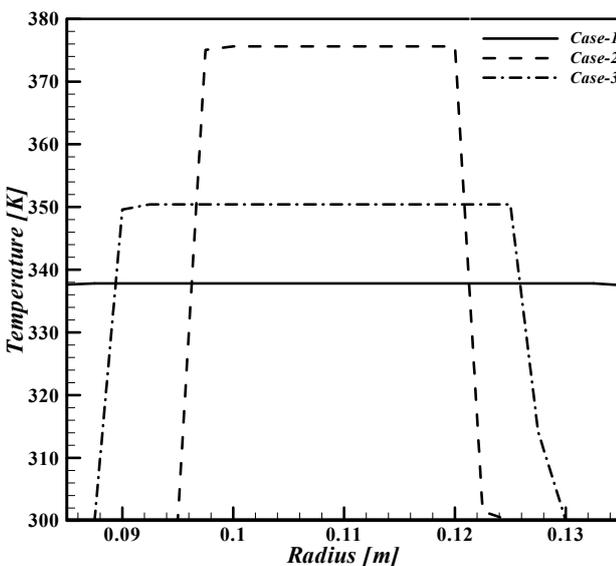**Fig. 9.** Variation of temperature with time at r_o (Parabolic pressure).

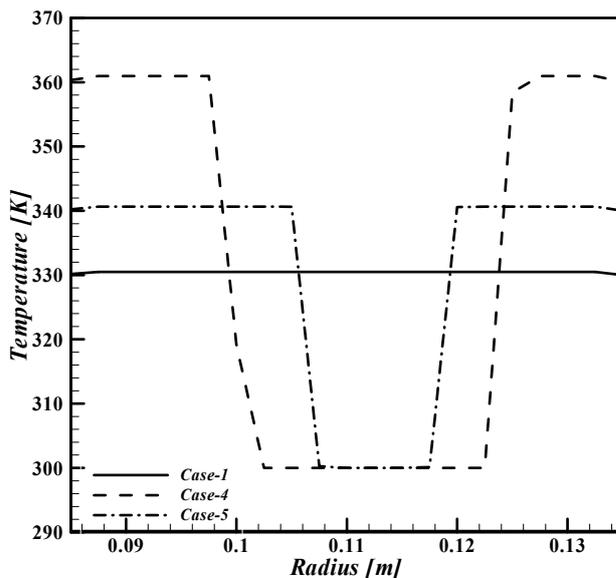**Fig. 10.** Variation of temperature with radius at t=0.1545 s (constant pressure).

Fig. 11. Variation of temperature with radius at t=0.492 s (Linear pressure).
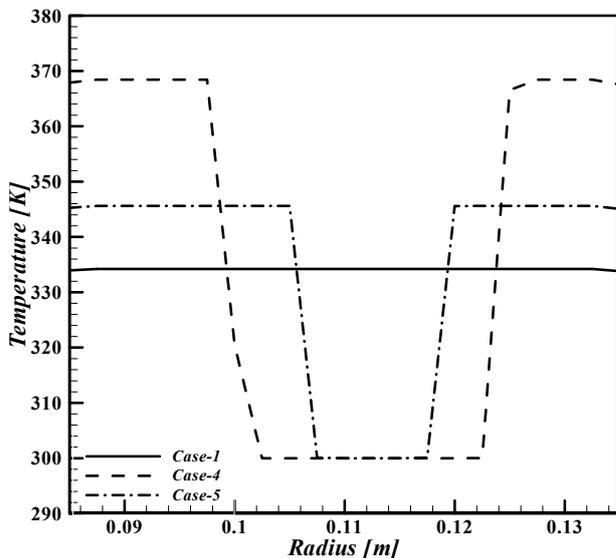

Fig. 12. Variation of temperature with radius at t=0.333 s (parabolic pressure).

Figures 10, 11 and 12 exhibit the surface temperature in the radial direction (between inner radius r_i and outer radius r_o). It can be noted that the temperature increases in the contact area of friction material (band contact) and no change in the other region of nominal frictional interface. This situation due to the fact of using low values of thermal conductivity for friction materials. The thermal variation will be just on the contact area, and which can be neglected for other regions of nominal frictional interface in case of band contact.

The normal operation of friction clutch makes repeated engagements and the maximum

temperature during this operation is very important. Temperature calculation has been made for repeated engagements made at regular intervals of time for the same energy dissipations. The time between engagements is taken 5 seconds. Figures 13, 14 and 15 show the variation of temperature with time at r_m for different types of pressure (constant, linear and parabolic) during 10 repeated engagements. The maximum temperatures reached after 10 engagements are 431 K, 415.3K and 423.3K corresponding to the constant pressure, linear pressure and parabolic pressure respectively.
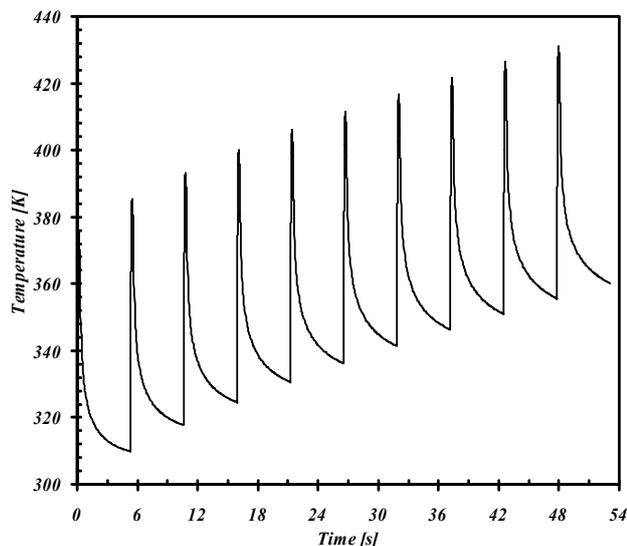

Fig. 13. Variation of temperature with time at r_m (Repeated engagements- constant pressure- case 2).
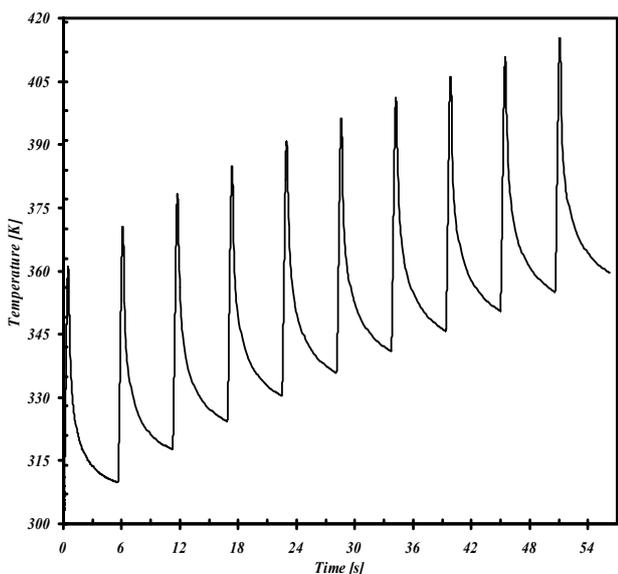

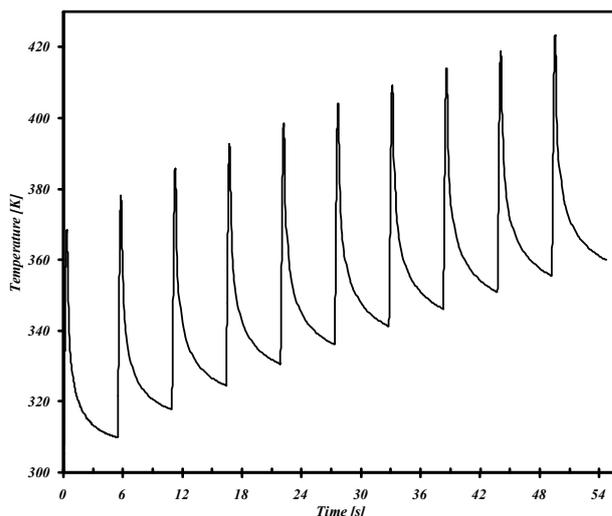**Fig. 14.** Variation of temperature with time at r_m (Repeated engagements- linear pressure-case 2).

Fig. 15. Variation of temperature with time at r_m (Repeated engagements- parabolic pressure- case 2).

5. CONCLUSIONS AND REMARKS

In this paper transient thermal analysis of dry friction clutch disc for a single engagement and repeated engagements based on the uniform wear theory was performed. Two-dimensional model was built to obtain the numerical simulation for band contact of disc clutch during slipping. The results show that both evolution of slipping time and contact area ratio are intensely effect disc clutch temperature fields in the domain of time. Proposed finite element modeling technique for three types of thermal loads depend on type of pressure (constant, linear and parabolic), and different region and location of band contact. It can be seen, that the result of temperature distribution for constant pressure type is higher than the other types of pressure, because of the total quantity of thermal load is applied in short time with compared to other types of thermal loads. Also, it can be noticed the uniform temperature on the contact surface because of the thermal load is constant in radial direction. The maximum temperature for constant, linear and parabolic pressures occur at ($t = 0.5t_{s1}$) (t = 0.78t_{s2}$) and ($t = 0.71t_{s3}$) respectively.

The study of temperature field of contact surfaces during repeated engagements operation is necessary to give indication about the maximum temperature, because of the temperature will increase rapidly when

327

increases number of times of engagements, and finally likely the temperature exceed the safe temperature, it's to leading the friction material to failure, before the expected lifetime of the clutch. The percentage of increases in maximum temperature are found 73.2 %, 89.1 % and 80.2 % corresponding to the constant pressure, linear pressure and parabolic pressure respectively when the number of engagement variation from (1 to 10), it is clear that the value of percentage increase of temperature for linear pressure type is higher the other types of pressure, this due to the total time for engagements when applied linear pressure is greater than the total time of engagements for other types.

The damaged or incorrectly machined flywheel (large deformation, thermal cracks ...etc) causes many of problems, one of them focusing the pressure on small regions of nominal frictional interface (e.g. bands and spots), for this it's essential when fitting a new clutch to a vehicle to ensure that the flywheel is in perfect condition in order to prevent any possible clutch problems. The minor scoring and grooving marks in flywheel can be removed by machining, but if the contact surface is deeply scored, the flywheel must be replaced.

Scoring and grooving prevent the driven plate from contacting the flywheel evenly, resulting in clutch shudder and slipping problems.

The band contact in clutches is considered one of the disadvantages, which produce by damaged flywheel, this type of contact lead to failure for the friction clutch material before estimated time of failure. The failure occurs in band contact due to concentration of frictional heating over zone smaller than frictional interface; this leads to a significant increase in the values of pressure, and then will generated temperatures higher than the expected values.

REFERENCES

[1] T.P. Newcomb: *"Calculation of Surface Temperatures Reached in Clutches when the Torque Varies with Time"*, J. of Mechanical Eng. Science, Vol. 3, No. 4, pp. 340-347, 1961.

[2] A.E. Anderson: *"Hot Spotting in Automotive friction Systems"*, J. of Wear, Vol. 135, No. 2, pp. 319-337, 1990.

[3] K. Lee, J.R. Barber: *"Frictionally Excited Thermoelastic Instability in Automotive Disk Brakes"*, ASME J. of Tribology, Vol. 115, pp. 607-614, 1993.

[4] K. Lee, J.R. Barber: *"An Experimental Investigation of Frictionally-Excited Thermoelastic Instability in Automotive Disk Brakes Under a Drag Brake Application"*, ASME J. of Tribology, Vol. 116, pp. 409-414, 1994.

[5] A.A. Yevtushenko, E.G. Ivanyk, O.O. Yevtushenko: *Exact formulae for determination of the mean temperature and wear during braking*, Heat and Mass Transfer, Vol. 35, No. 2, pp. 163–169, 1999.

[6] P. Decuzzi, G. Demelio: *"The effect of material properties on the thermoelastic stability of sliding systems"*, Wear, Vol. 252, No. 3-4, pp. 311–321, 2002.

[7] Yun-Bo Yi: *"Finite Element Analysis of Thermoelastodynamic Instability Involving Frictional Heating"*, ASME J. of Tribology, Vol. 128, No. 4, pp. 718-724, 2006.

[8] P. GRZEŚ: *Finite Element Analysis of Disc Temperature during Braking Process*, acta mechanica et automatica, Vol. 3, No. 4, pp. 36-42, 2009.

[9] Xue Jing, Li Yuren, Liu Weiguo: *The Finite Element Model of Transient Temperature Field of Airplane Brake Disks with Rough Surface Profile*, in: *Proceedings of the IEEE International Conference on Automation and Logistics Shenyang*, China August 2009.

[10] P. Hwang, XWu, Y.B. Jeon: *Thermal–mechanical coupled simulation of a solid brake disc in repeated braking cycles*, in: *Proceedings of the Institution of Mechanical Engineers, Part J: Journal of Engineering Tribology*, Vol. 223, Part J: J. Engineering Tribology, 2009.

[11] Piotr GRZEŚ: *Finite Element Analysis of Temperature Distribution in Axisymmetric Model of Disc Brake*, acta mechanica et automatica, Vol.4, No. 4, pp. 23-28, 2010.

[12] Liuchen Fan, Xuemei Sun, Yaxu Chu and Xun Yang: *"Thermal-structure coupling analysis of disc brake"*, in: *2010 International Conference on Computer, Mechatronics, Control and Electronic Engineering (CMCE)*, 24 Aug - 26 Aug 2010, TBD Changchun, China.

[13] W. Nowacki: *Thermoelasticity*, Pergamon Press, Oxford, 1962.

[14] B. Czéla, K. Váradia, A. Albers, M. Mitariub: *"Fe thermal analysis of a ceramic clutch"*, J. Tribology International, Vol. 42, No. 5, pp. 714–723, 2009.

[15] R.W. Lewis, P. Nithiarasu, K.N. Seetharamu: *Fundamentals of the finite element*, Wiley, 2004.